



# Effect of Freeze-Thaw Cycle on Anchor Fracture Load in Carbonate Rocks

Sevgi Çetintaş<sup>1\*</sup>, Sercan Serpinli<sup>2</sup>

<sup>1</sup>Vocational School of Technical Sciences,  
Akdeniz University, Antalya, 07058, TURKEY

<sup>2</sup>Mining Engineer, Antalya, 07000, TURKEY

\*Corresponding Author

DOI: <https://doi.org/10.30880/ijscet.2023.14.04.029>

Received 27 April 2023; Accepted 18 December 2023; Available online 28 December 2023

**Abstract:** Natural stone is widely used as a cladding material in the construction sector due to its durability and aesthetic appearance. When anchoring natural stone to building exteriors, it is of great importance to consider the mineralogical and mechanical properties of the stone. This study examines the changes in the breaking loads at the dowel holes of different carbonate stones used as cladding material in relation to freeze-thaw cycles and identifies the relationship of such changes with the physical and mechanical properties of the samples. For this purpose, four different types of natural stones were acquired, and the breaking loads at the dowel holes of the stone samples were analyzed according to standard procedures after being subjected to 25 freeze-thaw cycles. Mineralogical, petrographic, physical and mechanical characteristics of the stone samples were identified. It was shown that the breaking load values obtained at the anchorage points decreased due to the freeze-thaw cycles, and that the physical, mechanical and mineralogical characteristics of the sample had an effect on breakage.

**Keywords:** Breaking load, dowel, natural stone, freeze-thaw

## 1. Introduction

Natural stones are a material used among architects and builders because of their durability and aesthetic appearance. They are widely used as both cladding and flooring materials due to their long-lasting nature in modern architecture. In recent years, the increase in urban construction and industrial developments have led to an increase in the use of natural stone as an exterior cladding material for buildings, and different installation methods have been developed. The installation of natural stone slabs requires the use of mortar or mechanical fixings. In the mortar method, natural stone slabs are attached to the walls of the building using a cement mortar, while mechanical installations involve the fixture of natural stone slabs using hook systems made from stainless steel or galvanized metal components known as “anchors”. The approach to cladding buildings using natural stones fixed on mechanical installations has recently been referred to as the ventilated façade (Camposinhos, 2014; Camposinhos et al., 2008). This method allows for the future replacement or repair of slabs without damaging the facade of the building. Given the greater risk associated with falling materials with natural stone cladding with the increase in building heights, it is widely accepted that it is safer to install slabs on carriers and hooks (Loughran 2007; Gürani and Canbolat 2012).

There are numerous parameters to be taken into account when selecting natural stone as a cladding material, including the physical, mechanical, mineralogical and petrographic characteristics of the stone, the installation method and the prevailing atmospheric effects (wind, heat, humidity). Previous studies have investigated the parameters that play a key role in the cladding of buildings. The study by Camposinhos (2011) focused on the bending strength and

breakage loads of widely used natural stone, exploring the differences between the anchorage methods through “dowel” and “undercut” anchorage experiments. The size of the natural stone slabs used in exterior cladding and the anisotropic planes are crucial parameters that should be considered. Gürcan (2014) investigated the breaking loads of marble, limestone and granite samples of different thicknesses to be used in facade cladding. The study by Pires et al. (2011) examined the relationship between bending strength and anchorage system when using cladding materials (slate) with anisotropic plane in exterior cladding applications, as well as the importance of the bending behaviors of materials used for exterior cladding exposed to wind and physical impacts (Camposinhos and Camposinhos 2009; Moreiras et al., 2008; Camposinhos 2012). Siegesmund et al. (2008) explored the change in bending behaviors of buildings clad with natural stone in relation to changes in humidity and temperature and grain sizes. A further study examined the effect of environmental factors (heating and cooling) on the pliability of granite and identified the type and extent of bending when used as a cladding material, and the authors highlighted that the bending of granite boulders was associated with the interaction between mineral phases during thermal weathering and the presence of water (Siegesmund et al., 2008). In a similar study, seeking to identify the internal and external factors that should be taken into account to reduce and prevent biological damage to cladding stone. These materials used as well as the environmental conditions (rain, wind, humidity, temperature, atmospheric pollution, etc.) to which they would be exposed were analyzed. The authors noted that all internal factors should be taken into consideration to ensure that organic and inorganic particles do not settle in buildings, and that such properties as thickness, surface form and the geometry of the material used should be designed considering ambient conditions (López and Alonso 2010). Moreover, factors such as the structural design of the cladding system, the corrosion of the fixtures (dowel points and fastening elements) and their incompatibility with the materials used give rise to such problems as the bending, fracture and falling of materials (West and Heinlein 2000; Ivorra et al., 2013). The authors further examined the breaking loads and the manner of breakage sustained after loads were applied to steel pins of three different diameters in granite cladding. It is important to understand the damage behavior of such fastenings (Huang et al. 2020). In the literature, although the service life (duration) of natural stone attached with anchorage systems and the effects of the physical, mechanical and mineralogical properties have been examined separately in many different studies, there has been little research undertaken to date on the breaking load of natural stone installed with anchorage systems in relation to freeze-thaw cycles in tandem with physical, mechanical and mineralogical properties of the natural stone. Rocks in cold climates are always exposed to day-night freeze-thaw cycles and are within a certain stress field, and this formation environment has a significant impact on the mechanism behind rock deformations and failure (Lie and Lie 2014). As a result of the freezing of the water settled in the pores of the rocks, the pressure increases in the pores and micro-cracks occur (Bell, 1983). The physical weathering that occurs depending on the length of the freeze-thaw cycle number of freeze-thaw cycles affects the strength of rocks in the long term (Chen et al., 2004).

The present study explores the changes in the physical, mechanical and mineralogical properties of natural stone by determining the breaking load values at dowel hole points after freeze-thaw cycles.

## 2. Materials and Methods

For the experimental part of the study, four types of natural metamorphic and sedimentary stone were procured from different marble processing plants. To determine the change in the breaking load of the samples at the dowel holes after freeze-thaw cycles, the standards related to the determination of breaking loads at dowel holes (TS EN 13364) and determination of frost resistance (TS EN 12371) were taken into consideration. To determine the breaking load at the dowel holes, three 20 x 20 x 3 cm samples were taken from each stone specimen, holes with a diameter of  $10\pm 0.5$  mm and a depth of  $30\pm 2$  mm were drilled using a pillar drill with no hammer motion (Fig.1), and the dowel pins were fixed into the holes using CEM I 52.5 R cement (Fig. 2).



**Fig. 1 - Drilling the dowel hole**

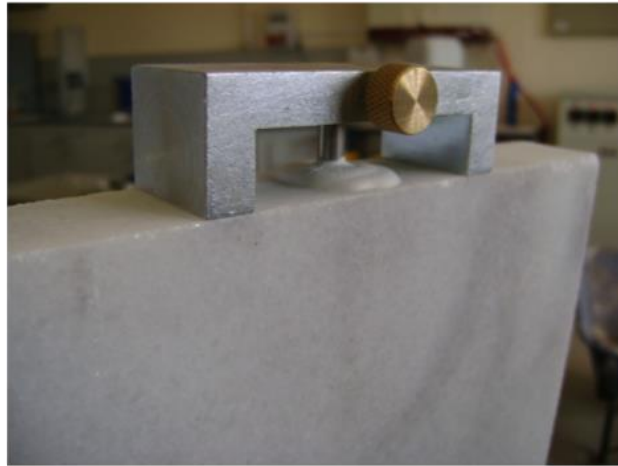


**Fig. 2 - Fixing the pin**

The prepared samples were kept at  $25 \pm 5$  °C for a minimum of 48 hours before the experiment for the concrete to set in the dowel holes. To determine the breaking loads at the dowel holes after frost, the samples were tested according to the TS EN 12371 standard. The samples with the concreted dowel holes were kept in water for 48 hours and then placed in the cabinet of a freeze-thaw tester. The samples were then subjected to a total of 25 cycles involving six hours of freezing at  $-12$  °C, for which the samples were immersed in water, followed by six hours of thawing in water at  $20$  °C. At the end of the 25th cycle, the samples were removed from the tester and subjected to constant weighing at a temperature of  $70 \pm 5$  °C. The breaking load (F, N) at the dowel holes of the samples that had completed their freeze-thaw cycle was determined by applying a speed of  $50 \pm 5$  N/s perpendicular to the dowel axis (Fig. 3). The greatest distance from the center of the dowel hole to the edge of the fracture (bA) and the distance from the hole to the surface in the direction of the applied force (d1) were then measured.

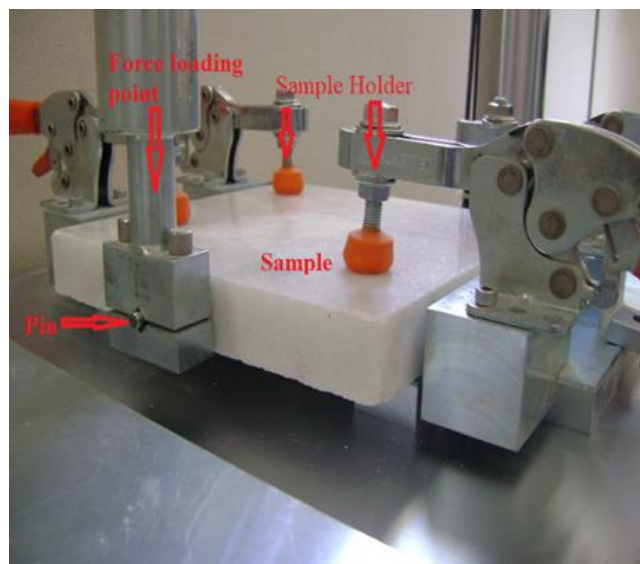


**Fig. 3 - Breaking load setup**

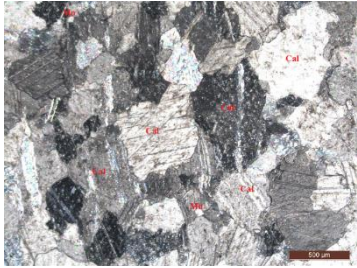
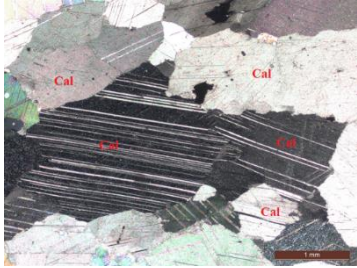
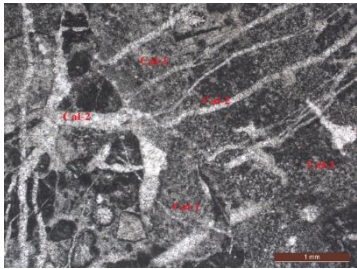
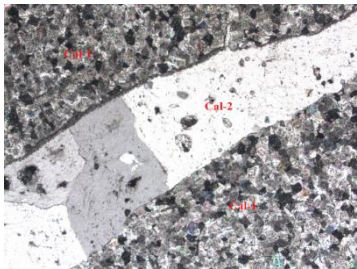
For the characterization tests, the mineral composition and micromorphological characteristics of the natural stone samples were examined in detail using a Nikon Eclipse 2V100POL polarizing microscope. The tests conducted to determine the physical and mechanical properties of the natural stone samples include microhardness (TS EN 14205), Schmidt hardness (ISRM 1981), compressive strength (TS EN 1926), flexural strength under concentrated load (TS EN 12372), flexural strength under constant moment (TS EN 13161) and point load strength (ISRM 1981).

### 3. Results and Discussion

#### 3.1 Petrography and Mineralogy

The thin section images obtained from polarizing microscope examinations and the grain size measurements are given in Table 1. Calcite was the predominant mineral in the marble samples, although details of secondary calcite and crack widths in the limestone samples are also included.

**Table 1 - Mineralogical and petrographic description of the samples**

Sample Code (Commercial Name)	Microscopic identification	The PLM Photos of the samples	The Macroscopic images of samples
M1 (Afyon Sugar)	Rock Name: Marble Calcite width (µm ): Avr.: 337.12 Max: 831.68 Min: 85.14		
M2 (Muğla White)	Rock Name: Marble Calcite width (µm ): Avr.: 947.54 Max: 2319.2 Min: 247.31		
K1 (Bilecik Beige)	Rock Name: Limestone Calcite width (µm ): Avr.: 7.65 Max: 72.4 Min: 1.86 Secondary calcite width (µm): Avr.: 80.38 Max: 646.16 Min: 7.41 Crack width (µm): Avr.: 418.46 Max: 1639.94 Min: 11.24		
K2 (Light Emperor)	Rock Name: Dolomitic Limestone Calcite width (µm ): Avr.: 114.48 Max: 218.98 Min: 27.17 Secondary calcite width (µm): Avr.: Max: Min: Crack width (µm): Avr.: 1281.56 Max: 1630.05 Min: 785.18		

Calcite was found to be the most prevalent mineral in samples M1 and M2 of metamorphic origin, and was also the predominant mineral in sample K1 of sedimentary origin, while the predominant mineral in sample K2 was dolomite. The analysis of sample M1 showed that the rock consisted of microcrystalline calcites and had a granoblastic texture. The average grain size of calcite was 337.12  $\mu\text{m}$ . Limonite and manganese, known as earth pigments, were identified on the surfaces of the small-sized calcite crystals located on the crystal boundaries. The examination of sample M2 revealed it to consist of calcite with perfect cleavage. Calcite crystals are euhedral and their crystal boundaries pronounced, and the average calcite grain size measured was 947.54  $\mu\text{m}$ . The calcite crystals that made up the rock were observed to have a homogeneous distribution. The examination of limestone sample K1 revealed the rock to consist of microcrystalline calcite. The cracks that had formed in this sample were found to have filled with secondary calcite crystals of different sizes. The average grain size of calcite was 7.65  $\mu\text{m}$ , the average grain size of secondary calcite was 80.38  $\mu\text{m}$  and the average crack width was 418.46  $\mu\text{m}$ . A microscopic examination of sample K2 showed that the rock consisted of dolomite, and a secondary dolomite formation was observed in the cracks. The measured grain size of calcite was 114.48  $\mu\text{m}$  and the average crack width was 1281.56  $\mu\text{m}$ . An analysis of this mosaic-textured sample revealed the dolomite to be anhedral, and the cleavage of the mineral grains were not well developed. Minerals have been reported to play an important role in the weathering of rock due to freeze-thaw cycles. Although minerals such as calcite and/or dolomite that make up natural stones have a very simple mineralogical composition, their weathering properties are manifold (Siegesmund et al., 2008). The changes in the breaking loads at the dowel holes, the maximum breaking length and the distance from the hole to the surface after freeze-thaw cycles suggest that mineralogical properties play a key role in determining the breaking loads at dowel holes after freeze-thaw cycles, although it can be suggested that the filling of capillary cracks and thicknesses also play a role in this process.

### 3.2 Breaking Load, Maximum Distance ( $b_A$ )

The dowel hole tests to identify the breaking load of the samples used in the study were carried out under laboratory conditions after the freeze-thaw cycles. The arithmetic averages of the values obtained from the tests are presented in Table 2. As can be seen in Fig. 4, the breaking load values of the samples were varying between 1.45 kN and 1.60 kN in the laboratory environment (unprocessed samples). The fracture load values of the samples were obtained between 0.79 kN and 1.46 kN after freezing and thawing cycles. While the highest fracture load value was obtained in the K1 sample, was followed by the K2, M1 and M2 samples, respectively. As to the rates of change in the samples after freeze-thaw cycles, the highest rate of change was observed in sample M2 at 50.38%, while the lowest rate of change was noted with K2, which decreased by 5.02%.

**Table 2 - Breaking load ( $F_{b1}$ ), maximum distance ( $b_A$ ) and distance from the hole to the surface ( $d_1$ ) before and after freeze-thaw cycles**

Sample Code	Before Freeze-Thaw			After Freeze-thaw		
	$F_{DH}$ (kN)	$d_1$ (mm)	$b_A$ (mm)	$F_{DH}$ (kN)	$d_1$ (mm)	$b_A$ (mm)
M1	1.52	10.01	36	1.16	9.47	36.96
M2	1.60	10.01	33	0.79	8.43	38.64
K1	1.56	10.40	40.9	1.46	9.75	37.94
K2	1.45	10.04	34.7	1.38	11.31	68.05

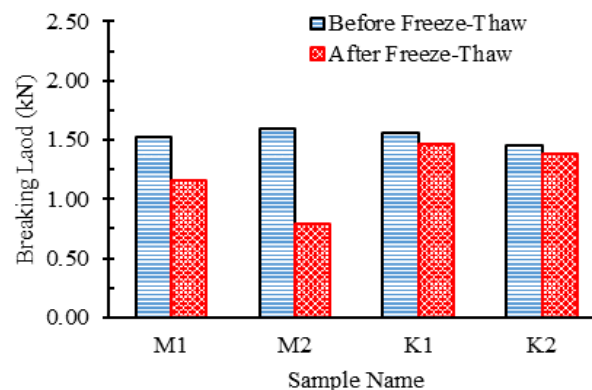


**Fig. 4 - Breaking load of the samples under normal conditions and after freeze-thaw cycles**

Previous studies have reported that during the freeze-thaw cycles of natural stone, the rock structure, the presence of cracks and the porosity ratio plays an important role in the process behind the transformation of water into ice crystals. The rock structure is defined by its texture and the interlocking of crystals, and such rock parameters have been reported to control the resistance of the material to the development of stress in the pores (Ruedrich et al., 2011). In the freeze-thaw cycle, the volumetric increase during the transition of water to ice can reduce the interlocking of crystals and/or can lead to new cracks, which may also be related to the mineralogical properties of the rock. For example, the minerals in sample M2 are euhedral, its grain size is larger than that of other samples and its grain boundaries are pronounced, and these resulted in more calcite grains being broken down due to freeze-thaw cycles. This gives rise to the formation of micro gaps and cracks, resulting in decreased strength. The fact that the K1 sample has a cracked structure and secondary calcite crystals of different sizes are found in the cracks will cause a decrease in the strength of the rock during the freeze-thaw cycles. Because, during the freeze-thaw cycle process, small pores and micro-cracks begin to grow and decompose the limestone samples, causing a decrease in strength. The greatest distances from the hole to the edge of surfaces of the samples used in the study are presented in Fig. 5. As can be seen in Fig. 5, the greatest distance to the edge of the fracture in the untreated samples varied between 33 mm and 40.9 mm, while these figures were in the 36.96–68.05 mm range after the freeze-thaw cycles. The rate of change of  $b_A$  was found to increase by 2.67%, 17.09% and 96.11% in samples M1, M2 and K2, respectively, and to decrease by 7.24% in sample K1. It is thought that the change obtained in the longest distance from the fracture edge on the surface of the samples is due to the deterioration of the grain boundaries of the minerals forming the rock as a result of the freeze-thaw cycles. In addition, bonding with the cement and rock used to fix the stud rod is also effective in obtaining these values. Following the tests, no significant change was observed in the distance from the hole to the surface ( $d_1$ ) in the untreated samples, while differences were observed after the freeze-thaw cycles. The distance from the hole to the surface ( $d_1$ ) in the untreated samples ranged from 10.01 mm to 10.40 mm, while the values obtained after the freeze-thaw processes varied between 8.43 mm and 11.31 mm (Fig.6).

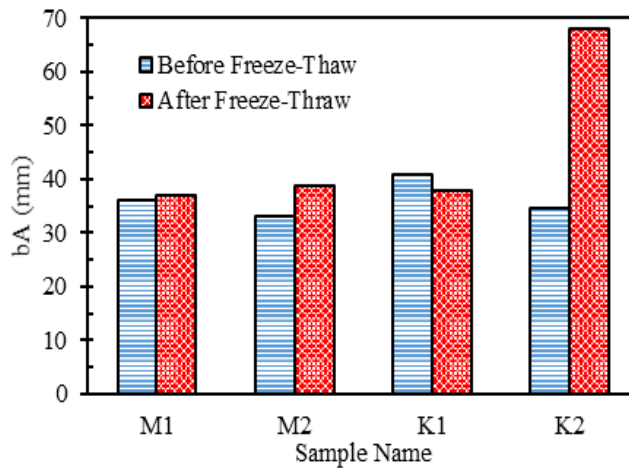


Fig. 5 -  $b_A$  of the samples under normal conditions and after freeze-thaw cycles

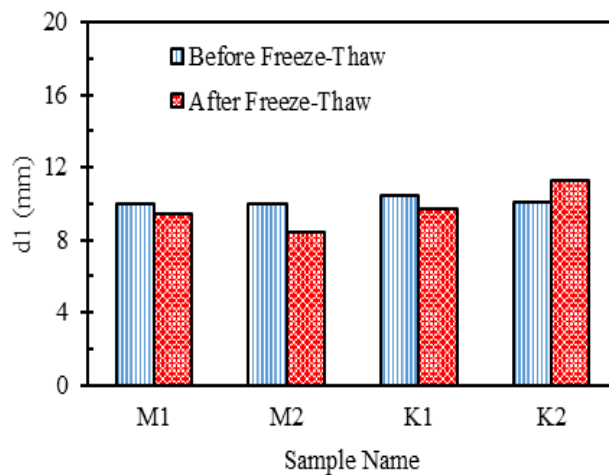


Fig. 6 -  $d_1$  of the samples under normal conditions and after freeze-thaw cycles

As to the rate of change after the freeze-thaw cycles, the  $d_1$  of samples M1, M2 and K1 decreased by 5.39%, 15.78% and 6.25%, respectively, while the  $d_1$  of sample K2 increased by 12.65%. In rocks and other porous geomaterials, the effects of freeze-thaw cycles and fatigue loading have been identified in previous studies as two main factors leading to the gradual degradation of the material (Wang et al., 2021; Wang et al., 2020). Moreover, Martínez-Martínez et al. (2013) highlighted that the pattern of rock weathering under freeze-thaw conditions was clearly nonlinear, suggesting the onset of sample destruction (weathering) from the moment cracks form and spread rapidly (critical threshold of weathering) (Martínez-Martínez et al., 2013). It is emphasized that this critical threshold is reached after a different number of freeze-thaw cycles for each type of rock, and that the values of both the longest distance to the edge of the fracture ( $b_A$ ) and the distance from the hole to the surface ( $d_1$ ) vary, attributable both to the critical threshold of weathering of each natural stone and loading fatigue.

### 3.3 Physical and Mechanical Properties

The freeze-thaw cycles effect is an important in natural stone factor, its can lead to gradual weathering and causes the rocks to exhibit different damage mechanisms depending on their physical - mechanical properties. The arithmetic mean results obtained from the physical and mechanical tests of the samples used in this study are given in Table 3.

**Table 3 - Physical and Mechanical results of samples**

(WA: water absorption, MH: microhardness, PL: Point load, SH: Schmidt hardness, CS: Compressive strength, Flx 3: Flexural strength-3 point, Flx 4: Flexural strength-4 point)

Sample Code	WA (%)	MH (HK)	PL (kN)	SH	CS (MPa)	Flx-3 (MPa)	Flx-4 (MPa)
M1	0.09	147	8.30	55.00	107.40	8.40	12.20
M2	0.13	135	7.50	54.00	75.53	8.33	8.74
K1	0.21	164	8.50	60.00	134.90	8.54	8.95
K2	0.80	347	11.80	68.00	148.10	4.85	5.37

Among the physical properties of the samples, the microhardness value ranged from 135 to 347, and the SH rebound hardness value from 54 to 68. The sample with the lowest hardness value was identified as M2, while K2 provided the highest hardness value. Among the mechanical properties, compressive strength values ranged from 75.53 to 148.10 MPa. It was observed that the compressive strength of sample K2, the calcite crystals of which were small and the cracks were narrow, was higher than that of the other samples. The flexural strength of the samples under constant moment ranged from 4.85 to 8.54 MPa, while their flexural strength under a concentrated load ranged from 5.37 to 12.20 MPa. The results of the point load strength test revealed a highest value of 11.80 and a lowest value of 7.50.

Simple linear regression analyses were made of each parameter with an attempt to identify the relationship between the variables involved in the breakage of the samples used in the anchorage applications in relation to the freeze-thaw cycles and some of their physical and mechanical properties. The resulting graphs reveal a linear relationship between breaking load and uniaxial compressive strength with a positive correlation of  $R^2=0.9148$ . (Fig. 7), although no significant correlation was identified between breaking load and microhardness, point load strength, and the Schmidt hardness and flexural strength values (three-point and four-point). The obtained values were  $R^2=0.262$ ,  $R^2=0.3561$ ,  $R^2=0.5073$ ,  $R^2=0.1323$  and  $R^2=0.0756$ , respectively (Fig.7). As to the relationship between the longest distance to the edge of the fracture due to the effects of freeze-thaw cycles ( $b_A$ ) and the physical and mechanical properties of the samples, a positive linear correlation was identified between  $b_A$  and microhardness, between  $b_A$  and point load strength, and between  $b_A$  and Schmidt hardness, with  $R^2$  values of 0.9803, 0.9325 and 0.8279, respectively. However,  $b_A$  and flexural strength (three-point and four-point) have a high negative correlation ( $R^2=0.9960$  and  $R^2=0.7165$ ), as shown in Fig. 8. As flexural strength values increase, the longest distance to the edge of the fracture ( $b_A$ ) on the samples decreases.

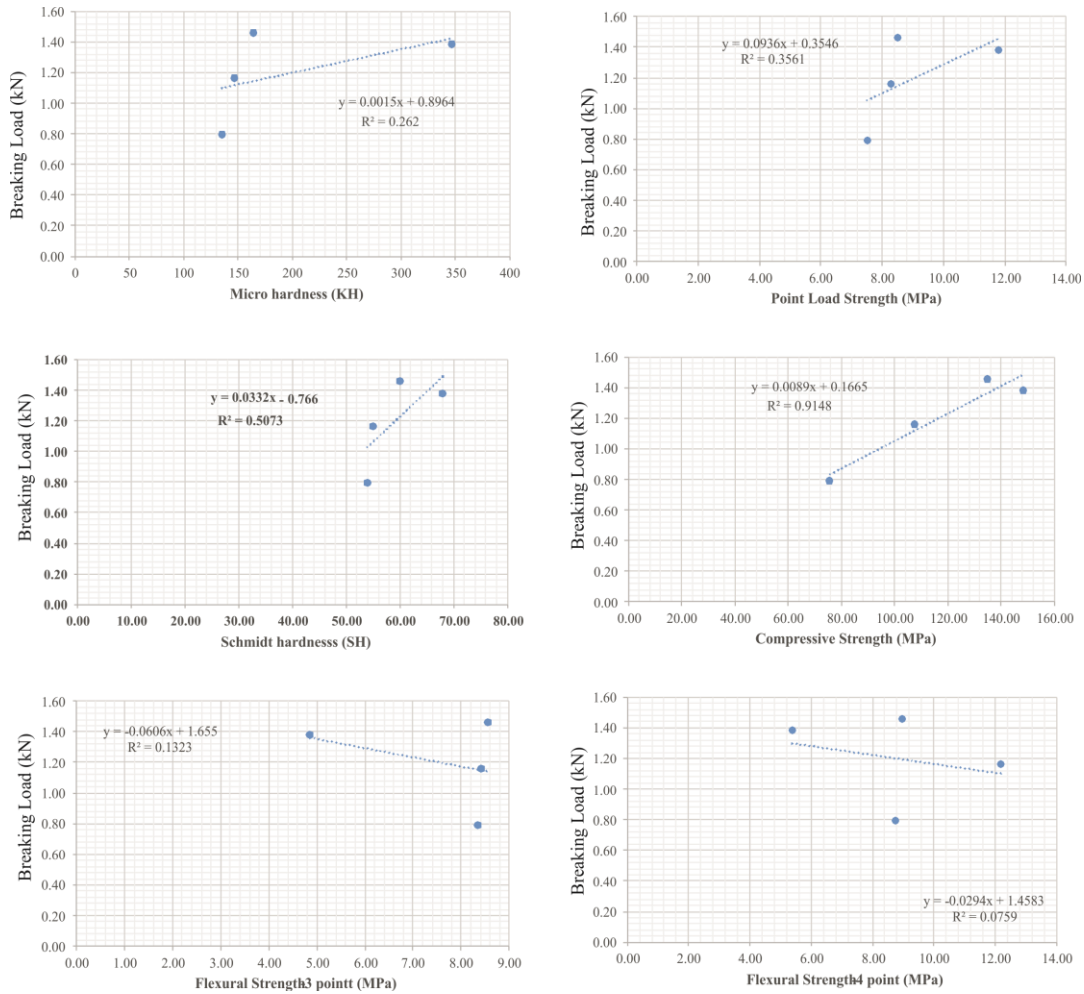


**Fig. 7 - Correlations between Breaking load to mechanical properties**

As to the relationship between the distance from the hole to the surface ( $d_1$ ) and the physical and mechanical properties of the samples, a positive linear correlation was similarly found between  $d_1$  and microhardness ( $R^2=0.8548$ ), between  $d_1$  and point load strength ( $R^2=0.93$ ), between  $d_1$  and Schmidt hardness ( $R^2=0.9076$ ), and between  $d_1$  and compressive strength ( $R^2=0.8512$ ). In contrast, a high negative correlation was found between  $d_1$  and flexural strength (three-point) with an  $R^2$  value of 0.7355, and a low negative correlation was found between  $d_1$  and the flexural strength (four-point) with an  $R^2$  value of 0.3899 (Fig.9). The obtained results suggest that significant relationships exist between the physical and mechanical properties and the distance to the edge of the fracture after the freeze-thaw cycle, as well as the distance from the hole to the surface. Studies of such relationships in different rock species is quite important. As noted in previous studies, irregular fracture angles and irregular fracture paths may be observed, depending on the characteristics of the rock (Song et al., 2021; Lammert and Hoigard 2007; Hébert et al., 2012). The marble and limestone samples exhibited different fracture paths after freeze-thaw cycles, which is an effect that depends entirely on the mineralogical, physical and mechanical properties of the rock. So, the critical threshold of weathering after freeze-thaw cycles also suggests an effect on the determination of the length of the fracture.

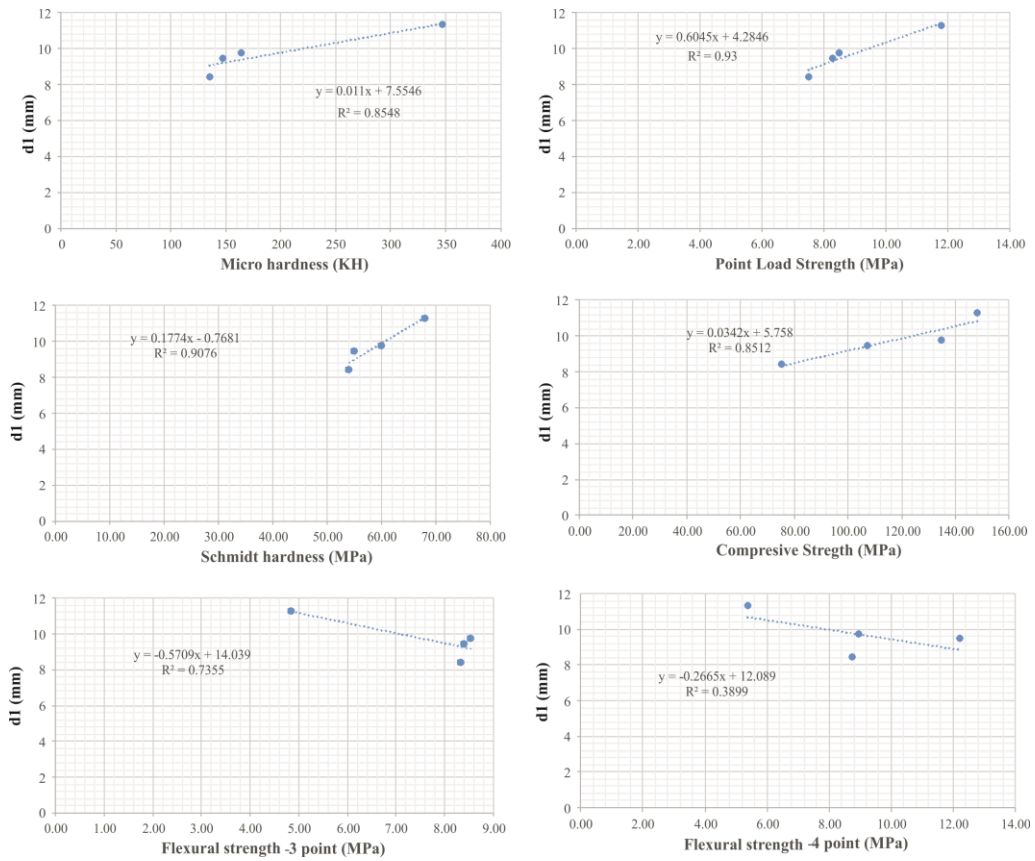


**Fig. 8 - Correlations between  $b_A$  and mechanical properties**

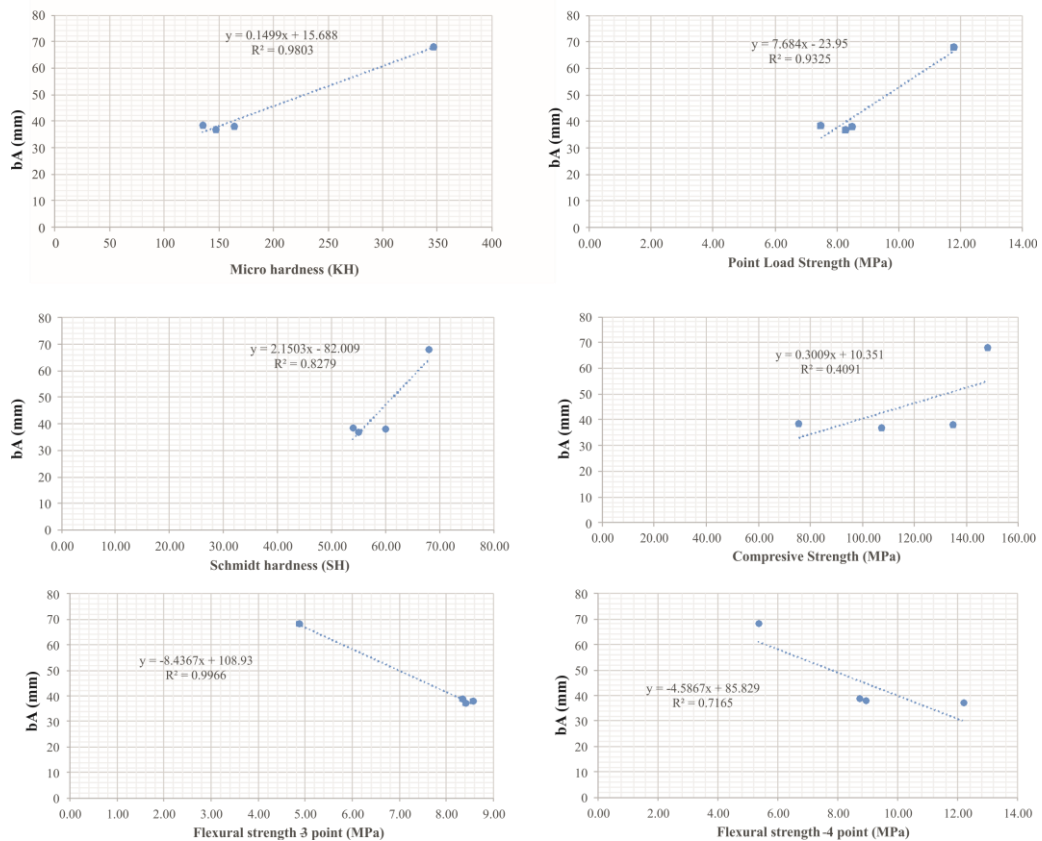


**Fig. 9 - Correlations between  $d_I$  and mechanical properties**

## 4. Conclusions

This study explores the change in breaking loads at dowel holes after freeze-thaw cycles in four natural stone specimens from different sources through an examination of their mineralogical, physical and mechanical properties. The results obtained from the experiments in the study are given below:

- The breaking load of the natural stones used in the study decreased after the freeze-thaw cycles, and these values were different for each sample.
- The value of  $b_A$  after the freeze-thaw cycles increased in the M1, M2 and K2 samples, but decreased in the K1 sample. The change in  $d_1$  was found to be similar to the change in  $b_A$ , and this is thought to be associated with the minerals that form the rocks, their size, the crack width and the crack filling, in that each rock has different weathering characteristics despite having a similar origin.
- A positive correlation was found between the breaking load and uniaxial compressive strength of the samples, while no significant correlation was noted between the breaking load and microhardness, point load strength, Schmidt hardness and flexural strength values (three-point and four-point).
- It was determined that the longest distance ( $b_A$ ) to the edge of the fracture that occurred due to the freeze-thaw cycles was associated with the physical and mechanical properties of the sample. A positive correlation was found between  $b_A$  and microhardness, point load strength and Schmidt hardness, while a high negative correlation was found between  $b_A$  and flexural strength (three-point and four-point).
- These results show that the freezing-thawing cycles of natural stones, which are exterior cladding materials used in buildings, are an important factor. Determining the properties of natural stones and using them in exterior cladding of buildings will ensure a longer life of the cladding material.

## Acknowledgement

We would like to thank TUBITAK for their financial support to Project No: 113M111.

## References

- Bell, F.G. (1983) *Engineering Properties of Soils and Rocks*, Butterworth & Co, ISBN 0-408-01457-1
- Camposinhos, R.S., Amaral, P.M., Rosa, L.G. & Pires, V. (2008) Dimension stone cladding design—dowel anchorage design. In: *2nd Int. Congress of Dimension Stones*, Carrara, Italy, pp.203-207, DOI: 10.13140/RG.2.1.2191.6008
- Camposinhos, R. & Camposinhos, R.S. (2009) Dimension-stone cladding design with dowel anchorage, *Construction Materials*, 162(3), pp.95-104, from doi:[10.1680/coma.2009.162.3.95](https://doi.org/10.1680/coma.2009.162.3.95)
- Camposinhos, R.S. (2011) Undercut anchorage in dimension stone cladding. *Construction Materials*, 166(3), pp.158-174, from doi:[10.1680/coma.11.00050](https://doi.org/10.1680/coma.11.00050)
- Camposinhos, R. (2012) Dimension stone design—Partial safety factors: A reliability based approach. *Construction Materials*, 165(3), pp.145-159, from doi:[10.1680/coma.10.00018](https://doi.org/10.1680/coma.10.00018)
- Camposinhos, R.S. (2014). *Stone Cladding Engineering*. Springer, [E-book] ISBN 978-94-007-6848-2, DOI 10.1007/978-94-007-6848-2
- Chen, C.H., Yeung, M.R. & Mori, N. (2004) Effect of water saturation on deterioration of welded tuff due to freeze-thaw action. *Cold Regions Science and Technology*, 38, pp.127–136, from doi:10.1016/j.coldregions.2003.10.001.
- Gürani, Y. & Canbolat, T. (2012) Different Approaches in the Use of Natural Stone at the Scale of Space from Past to Present. *Natural Life Natural Stone Symposium*, İstanbul, Turkey, pp.25-32 (In Turkish).
- Gürcan, S. (2014) Determination of Fracture Load in Dowel Hole of Natural Stones Used in Facade Cladding. Tubitak Project, Ankara, Turkey. Project number: 113M111, 2014.
- Hébert, R., Beouch, L., Fichet, O., Bigas J.P., Teyssié, D., Berthier, B. & Prichystal, J.B. (2012) Cracks and stains on facade-cladding made of carbonate rock thin panels. *Structural Survey*, 30(2), pp.130–144, from doi:10.1108/02630801211228734
- Huang, B., Fu, S., Lu, W. & Günay, S. (2020) Experimental investigation of the breaking load of a dowel-pinned connection in granite cladding, *Engineering Structures*, 215, 110642, from doi:[10.1016/j.engstruct.2020.110642](https://doi.org/10.1016/j.engstruct.2020.110642)
- ISRM (1981). *Rock Characterization, Testing and Monitoring –ISRM Suggested Methods*. Pergamon Press, 211
- Ivorra, S., García-Barba, J., Mateo, M., Pérez-Carramiñana, C. & Maciá, A. (2013) Partial collapse of a ventilated stone facade: diagnosis and analysis of the anchorage system. *Engineering Failure Analysis*, 31, pp.290–301, from doi:10.1016/j.engfailanal.2013.01.045
- Lammert, B.T. & Hoigard, K.R. (2007) Material strength considerations in dimension stone anchorage design, in *Dimension stone use in building construction*, pp.40-57, from doi:10.1520/STP45363S
- Liu, Q. & Liu, X. (2014) Research on critical problem for fracture network propagation and evolution with multifold coupling of fractured rock mass. *Rock and Soil Mechanics* 35(2), pp.305 – 320.

- Loughran, P. (2007) Failed Stone: Problems and Solutions with Concrete and Masonry. *Birkhäuser Architecture*, from doi:10.1007/978-3-7643-8285-8.
- López, F.J.& Alonso, P. (2010) Ventilated façade of stone: factors that influence in the colonization of granite. *Global Stone Congress*, Alicante, Italy.
- Martínez-Martínez, J., Benavente, D., Gomez-Heras M., Marco-Castaño L.& García-del-Cura, M.A. (2013) Non-linear decay of building stones during freeze–thaw weathering processes. *Construction and Building Materials*, 38, pp.443–454, from doi:10.1016/j.conbuildmat.2012.07.059
- Moreiras, S.T.F., Paraguassu, A.B. & Ribeiro, R.P. (2008) Dimension stone for building facades: methodology for structural design. *Bulletin of Engineering Geology and the Environment*, 67, pp.53–57, from doi:10.1007/s10064-007-0103-4.
- Pires, V., Amaral, P.M., Rosa, L.G. & Camposinhos, R.S. (2011) Slate flexural and anchorage strength considerations in cladding design. *Construction and Building Materials*, 25(10), pp. 3966–3971, from doi:10.1016/j.conbuildmat.2011.04.029
- Ruedrich J., Kirchner D. & Siegesmund S. (2011) Physical weathering of building stones induced by freeze–thaw action: a laboratory long-term study. *Environmental Earth Sciences*, 63, pp.1573–1586, from doi: 10.1007/s12665-010-0826-6
- Siegesmund, S., Mosch S., Scheffzu, Ch. & Nikolayev, D. I. (2008) The bowing potential of granitic rocks: rock fabrics, thermal properties and residual strain. *Environmental Geology*, 55, pp.1437–1448, from doi: 10.1007/s00254-007-1094-y
- Siegesmund S., Mosch S., Scheffzük Ch. & Nikolayev, D.I. (2008) The bowing potential of granitic rocks: rock fabrics, thermal properties and residual strain. *Environmental Geology*, 55, pp.1437–1448, from doi:10.1007/s00254-007-1094-y
- Song, Z., Wang, Y., Konietzky, H., Cai X. (2021) Mechanical behavior of marble exposed to freeze-thaw-fatigue loading. *International Journal of Rock Mechanics and Mining Sciences*, 138, 104648, from doi:10.1016/j.ijrmmms.2021.104648
- Turkish Standardization Institute (2003). *Natural stone test methods - determination of the breaking load at dowel hole*. Ankara: TS EN 13364
- Turkish Standardization Institute (2003). *Natural stone test methods - Determination of frost resistance*. Ankara: TS EN 12371
- Turkish Standardization Institute (2003). *Natural stone test methods - Determination of Knoop hardness*. Ankara: TS EN 14205
- Turkish Standardization Institute (2000). *Natural stone test methods - Determination of uniaxial compressive strength* Ankara: TS EN 1926
- Turkish Standardization Institute (2001). *Natural stone test methods - Determination of flexural strength under concentrated load*. Ankara: TS EN 12372
- Turkish Standardization Institute (2003). *Natural stone test methods-Determination of flexural strength under constant moment*. Ankara: TS EN 13161
- Wang, Y., Gao, S.H., Li, C.H.& Han, J.Q. (2020) Energy dissipation and damage evolution for dynamic fracture of marble subjected to freeze-thaw and multiple level compressive fatigue loading. *International Journal of Fatigue*, 142, 105927, from doi:10.1016/j.ijfatigue.2020.105927.
- Wang, Y., Feng, W.K., Wang, H.J., Li, C.H.& Hou, Z.Q. (2020) Rock bridge fracturing characteristics in granite induced by freeze-thaw and uniaxial deformation revealed by AE monitoring and post-test CT scanning. *Cold Regions Science and Technology*, 177, 103115, from doi: 10.1016/j.coldregions.2020.103115.
- West, D.G.& Heinlein M. (2000) Anchorage pull out strength in granite: design and fabrication influences. In: Hoigard KR, editor. *Dimension stone cladding: design, construction, evaluation, and repair*, ASTM STP 1394. West Conshohocken (PA): American Society for Testing and Materials (ASTM), pp. 121–134.